Temperature-Insensitive (K,Na)NbO_3-Based Lead-Free Piezoactuator Ceramics

Ke Wang, Fang-Zhou Yao, Wook Jo, Danka Gobeljic, Vladimir V. Shvartsman, Doru C. Lupascu, Jing-Feng Li, and Jürgen Rödel*

The development of lead-free piezoceramics has attracted great interest because of growing environmental concerns. A polymorphic phase transition (PPT) has been utilized in the past to tailor piezoelectric properties in lead-free (K,Na)NbO_3 (KNN)-based materials accepting the drawback of large temperature sensitivity. Here a material concept is reported, which yields an average piezoelectric coefficient d_{33} of about 300 pC/N and a high level of unipolar strain up to 0.16% at room temperature. Most intriguingly, field-induced strain varies less than 10% from room temperature to 175 °C. The temperature insensitivity of field-induced strain is rationalized using an electrostrictive coupling to polarization amplitude while the temperature-dependent piezoelectric coefficient is discussed using localized piezoresponse probed by piezoforce microscopy. This discovery opens a new development window for temperature-insensitive piezoelectric actuators despite the presence of a polymorphic phase transition around room temperature.

1. Introduction

Actuator applications require electromechanical coupling providing high strain with high force, e.g., fuel injectors, ink cartridges, ultrasonic motors, etc.[1] This requirement is largely fulfilled by piezoelectric materials, which allow direct conversion between electrical and mechanical energy. At present, lead zirconate titanate (PZT)-based ceramics are the most widely used materials for piezoelectric actuators.[2] According to a survey for piezoelectric actuators in the year 2009, PZT-based bulk ceramics accounted for about 98% of the entire revenue, which is as large as 6.6 billion US dollars.[3] Despite its adaptability to a wide range of distinct applications, PZT contains a large portion of hazardous lead, raising health and environmental concerns, as addressed in international regulations such as WEEE (waste of electrical and electronic equipment) and RoHS (restriction of certain hazardous substances). Therefore, tremendous efforts have been devoted to the development of competitive lead-free counterparts during the past decade.[4–12] The breakthrough made by Saito et al. in highly textured KNN-based ceramics with co-dopants of Li, Ta, and Sb has offered a significant impact on the development of lead-free piezoceramics.[4] Hence, unprecedented attention is focused on to KNN after its first discovery more than 50 years ago.[13] Despite the fact that pure KNN ceramics are normally associated with a poor piezoelectric coefficient d_{33} as low as 80 pCN^{-1},[13] the value reported by Saito et al.[4] reached up to 416 pCN^{-1}, comparable to that of soft PZT ceramics. Afterwards, numerous dopants were exploited in the KNN system geared towards improvement of the piezoelectric coefficient d_{33}, which could be conveniently measured using the quasi-static method (e.g., by a Berlincourt-meter). In contrast, the normalized strain $d_{33}^*(S_{max}/E_{max})$ has the same units, but is the property for actuator applications under large field excursions. Solid solutions with other species, such as $LiNbO_3$,[14] $LiTaO_3$,[15,16] etc. lead to advanced materials with piezoelectric coefficient d_{33} values in the range of 200–300 pCN^{-1}, while a comparably high piezoelectric coefficient d_{33} of 300–400 pCN^{-1} is also obtained at room temperature with special effort.[9,17–18]

Initially, dopants such as Li, Ta, and Sb were seen as being responsible for constitution of a morphotropic phase boundary (MPB) in KNN-based ceramics, mimicking that in PZT ceramics and eventually resulting in property enhancement.[14,15] Later on, it was proposed that the underlying origin for the property enhancement is not a classical MPB but a polymorphic phase transition (PPT), which exists in many materials such as in the classic perovskite $BaTiO_3$. In a heating cycle, pure KNN undergoes phase evolution from orthorhombic at room temperature to tetragonal around 220 °C, then further to cubic around 420 °C.[19] PPT theory suggests that the observed property enhancement in KNN-based ceramics is due to a shift of the tetragonal-orthorhombic polymorphic phase transition point ($T_{O\text{-}T}$) from about 220 °C to room temperature as a

Dr. K. Wang, F.-Z. Yao, Prof. J.-F. Li
State Key Laboratory of New Ceramics and Fine Processing
School of Materials Science and Engineering
Tsinghua University
Beijing 100084, P. R. China
E-mail: wang-ke@tsinghua.edu.cn
Dr. K. Wang, Dr. W. Jo, Prof. J. Rödel
Institute of Materials Science
Technische Universität Darmstadt
Darmstadt 64287, Germany
D. Gobeljic, Dr. V. V. Shvartsman, Prof. D. C. Lupascu
Institute for Materials Science
Universität Duisburg-Essen
Essen 45141, Germany

DOI: 10.1002/adfm.201203754

© 2013 WILEY-VCH Verlag GmbH & Co. KGaA, Weinheim

result of dopants.[16,20–22] Although there are still discussions on whether the orthorhombic phase in KNN-based system is actually monoclinic or not,[23–26] the influence of the PPT is more or less indisputable.

However, PPT is actually less favorable than MPB since it may result in problems of temperature sensitivity.[17,20,27,28] Zhang et al.[20] reported that for $LiSbO_3$ doped KNN ceramics, the normalized strain d_{33}*, dropped from 355 pmV^{-1} at room temperature to around 250 pmV^{-1} at 50 °C; while the radial coupling factor k_p also decreased linearly with increasing temperature above room temperature. Hollenstein et al.[28] demonstrated that the piezoelectric coefficient d_{31} and coupling factor k_p decreased up to 30% of their initial value after the first heating cycle up to 140 °C for Li-modified KNN. Akdoğan et al.[17] found that for $LiTaO_3$ and $LiSbO_3$ co-doped KNN ceramics the spontaneous polarization P_s, permittivity and piezoelectric coefficient d_{33} all peaked in a narrow temperature range at 25–31 °C. In order to improve the temperature stability, two possible solutions have been adopted so far: shifting the $T_{O\text{-}T}$ well below room temperature by chemical modifications,[22,27,29] or producing highly textured ceramic samples.[4,30] However, the former actually avoids the PPT problem by creating single tetragonal phase between room temperature and Curie point, which ineluctably sacrifices certainly piezoelectric activity (compared with those compositions benefiting PPT effect at room temperature); while the latter requires complex synthesis incompatible with mass production. As a result, the development of KNN-based ceramics is still hampered due to insufficient temperature stability.

In this paper, we report on promising KNN-based lead-free piezoceramics with enhanced strain behavior as well as remarkable temperature stability. The unipolar strain reaches 0.16% under an electric field of 6 kV mm^{-1}, sufficiently high for lead-free piezoceramics. Although the piezoelectric coefficient d_{33} demonstrates a temperature-dependent behavior, due to the existence of PPT effect, the unipolar strain retains its room-temperature value up to a temperature as high as 175 °C, suggesting promising potential for actuator applications. We introduce the new material first with a discussion of salient properties and then continue to highlight its properties in contrast to neighboring compositions.

2. Results and Discussion

2.1. Structure, Domain Evolution and Small Signal Properties

The nominal composition of the material of choice is $0.95(Na_{0.49}K_{0.49}Li_{0.02})(Nb_{0.8}Ta_{0.2})O_3$-$0.05CaZrO_3$ (CZ5) with 2 wt% MnO_2 addition, which is similar to a recently reported giant strain material engineered with duplex structure.[31] The X-ray diffraction (XRD) analysis describes the material as a solid solution with a perovskite structure, as shown in **Figure 1** a. Tiny traces of impurities are observed in the 2θ range between 20° to 40°, probably because that eight kinds of raw materials (including oxides and carbonates, see Experimental Section for details) are used for the synthesis and undesirable reactions between various species originate. The piezoelectric performance of KNN-based ceramics is especially sensitive to the perovskite phase structure, which can be quantified by assessing relative intensities of (002) and (200) peaks. For the orthorhombic phase, this ratio (I_{002}/I_{200}) is about 2:1, while turns to 1:2 for the tetragonal phase. [19] As for the present case, the (200) and (002) peaks are of similar magnitude, implying the coexistence of orthorhombic and tetragonal phases, with $T_{O\text{-}T}$ around room temperature. As mentioned before, dopants can lower $T_{O\text{-}T}$ in the KNN system. In the present study, it is most likely due to a collective effect of Li, Ta, and $CaZrO_3$. Note also that the (200) and (002) peaks are very close to each other, resembling a pseudocubic perovskite structure, which indicates promising piezoelectric performances.[32].

XRD data are routinely augmented by temperature-dependent dielectric properties to identify phase transitions in ferroelectrics. Two anomalies are observed in both permittivity and dielectric loss curves

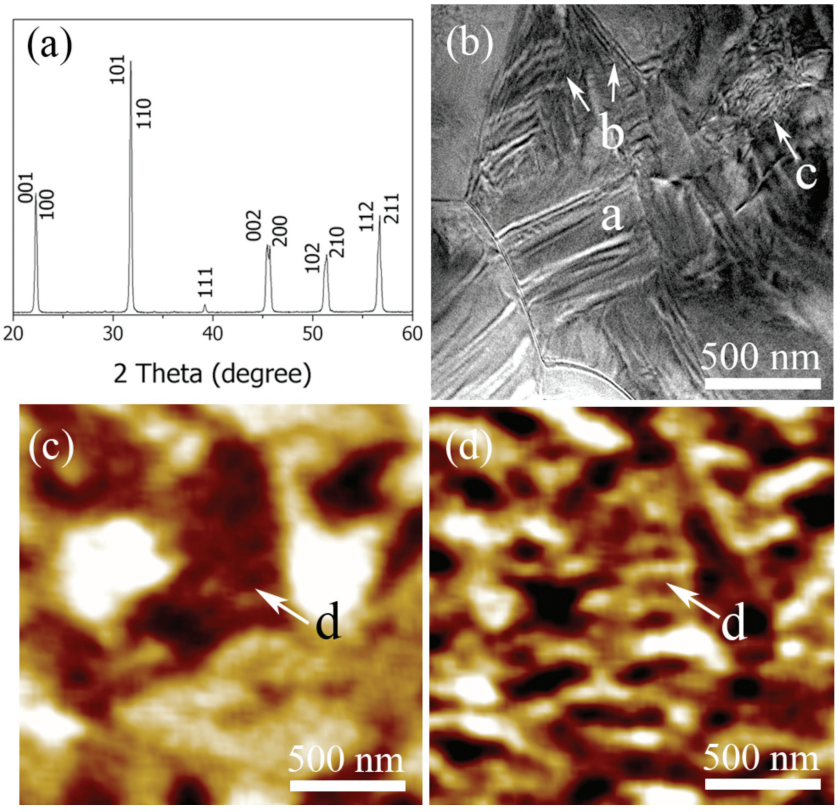

Figure 1. a) XRD pattern of CZ5 ceramics with peak indexing adopted for a tetragonal perovskite phase. b) TEM analysis of typical domain structures of CZ5. c) Vertical piezoresponse force microscopy (VPFM) image of domain structures of CZ5. d) Lateral piezoresponse force microscopy (LPFM) image of domain structures of CZ5.

© 2013 WILEY-VCH Verlag GmbH & Co. KGaA, Weinheim

Table 1. Representative piezoelectric coefficient d_{33} values obtained in non-textured KNN-based lead-free piezoceramics.

Material	d_{33} [pC N^{-1}]	Ref.
KNN	80	[13]
KNN+Li	324	[9]
KNN+Li, Ta, Sb (LF4)	300	[4]
KNN+Li, Ta, Sb	345	[17]
KNN+Li, Ta, Sb	380	[18]
KNN+Li, Ta+$CaZrO_3$	320	This study

(Figure S1, Supporting Information), respectively, indicating phase transitions of orthorhombic-tetragonal (at a broad transition range, $T_{O\text{-}T}$, between room temperature and 80 °C) and tetragonal-cubic (at T_C, 192 °C). The room temperature permittivity and dielectric loss measured at 1 kHz are 1735 and 0.014, respectively.

Superior piezoelectric properties were obtained for the poled CZ5 ceramics at room temperature. The piezoelectric coefficient d_{33} reached 320 pCN^{-1} (average of 270-360 pCN^{-1}), which is among the top values of d_{33} reported so far in non-textured KNN-based ceramics (see **Table 1**).[4,9,17,18] The radial coupling coefficient k_p is 0.47, which is also high in KNN-based lead-free piezoceramics. The mechanical quality factor Q_m at a value of 50 characterizes the current material as relatively "soft". Generally, the piezoelectric and electromechanical properties are comparable to soft PZT ceramics. Again, the orthorhombic-tetragonal co-existence is considered as a major reason for the excellent properties.[17] Microstructure analysis corroborated these findings. Typical domain structures of a poled ceramic sample are revealed by transmission electron microscopy (TEM) and piezoforce microscopy (PFM) studies, as depicted in Figure 1b–d. Due to the co-existence of orthorhombic-tetragonal phase structures, complex domain patterns are observed. Besides, the present study revealed a specific domain structure with both micro- and nanosized domains co-existing inside one single grain. As provided in Figure 1b, typical strip-like ferroelectric domains with width of several hundred nanometers are marked in area (a), in accordance with previous reports in KNN-based materials.[33–36] Meanwhile, area (b) and (c) demonstrate nanosized domains with irregular shapes, or featureless domains,[35] resembling similar nanodomains discovered in PZT ceramics at its morphotropic phase boundary.[37,38] Piezoresponse force microscopy (PFM) data are in accordance with TEM observations. Figure 1c,d demonstrate that relatively large 180° domains consist of strip-like quasi-periodical ferroelastic domains with period about 50–100 nm, see e.g., area (d). The observed domain patterns depend on grain size; large more regular domains were usually observed in bigger grains, while small irregularly shaped patterns were typical for fine grains (grain size distribution is visualized in Figure S2, Supporting Information). Domain size was found proportional to the square root of domain wall energy.[39] Since the energy of nanodomain walls is low, they would be easily reoriented under external excitations, e.g., applied electric field or mechanical force, resulting in high piezoelectric response. Actually, it has been suggested that nanodomains play a vital role in the high piezoelectric property in both lead-based[37,38,40] and lead-free perovskites,[18,41] which was further proven theoretically very recently.[10]

As our prime interest rests with temperature-dependent obtainable strain, temperature-dependent domain evolution is further addressed by PFM. For the unpoled sample, a reorganization of domain structures was observed in a temperature range between 140 °C and 160 °C. At higher temperatures domains start to disappear, and finally at 210 °C piezoresponse is almost zero. For the poled sample the vertical PFM (VPFM) displays unipolar contrast at room temperature as provided in **Figure 2**, implying a nearly ideal poling effect. This unipolarity is preserved up to the Curie point, while the magnitude of the vertical piezoresponse is fading away as temperature approaches T_C. At the same time, the lateral PFM (LPFM) images show more peculiar behavior. Comparison of the images taken at room temperature and at 127 °C demonstrates not only variation of the magnitude of lateral piezoresponse, but also changes of its sign (polarity) in the majority of grains. These changes indicate a reorganization of domain structure. Specifically the out-of-plane component of polarization (VPFM image) remains the same, but the in-plane component (LPFM image) rotates, and might be attributed to the orthorhombic-tetragonal phase transition between room temperature and about 80 °C.

2.2. Strain Behavior

Compared to a large number of reports concerning sensor-related issues in KNN-based ceramics (e.g., piezoelectric coefficient d_{33}), the strain behavior, as key feature for actuator systems,

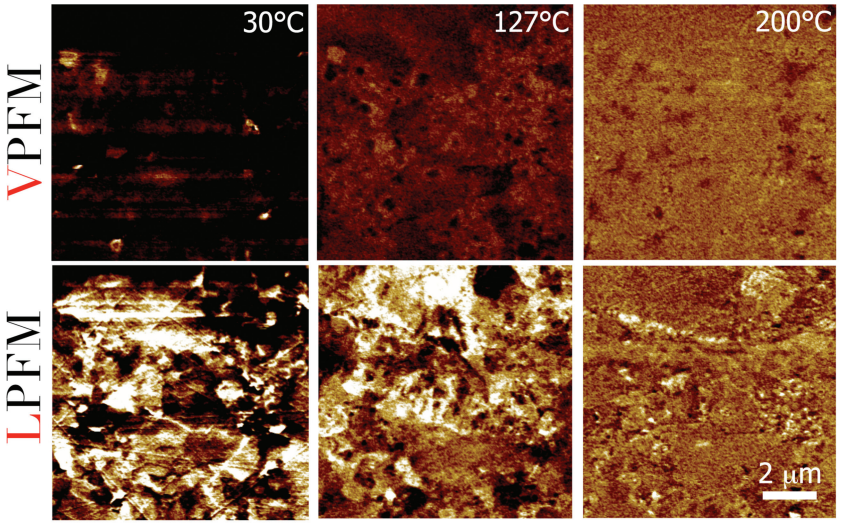

Figure 2. VPFM and LPFM images of the poled CZ5 sample surface as a function of temperature. The sample was poled in the vertical direction at room temperature using a Ag-paste electrode which was removed in an ultrasonic bath before PFM analysis.

© 2013 WILEY-VCH Verlag GmbH & Co. KGaA, Weinheim

is only occasionally targeted.[31] Typical strain values for soft PZT ceramics are around 0.15% at 2 kV mm^{-1}, while recently much higher strains up to 0.4% are obtained in a series of Bi-based materials resulting from field-induced relaxor-ferroelectric phase transition, though much higher fields (typically 8 kV mm^{-1}) are necessary.[3,7] In the present study the strain reaches 0.16% at 6 kV mm^{-1} (Figure S3, Supporting Information), which is a very promising value for ceramic samples, compared to lead containing PZT piezoceramics, and electrostrictive ceramics, such as Pb(Mg, Nb)O_3-$PbTiO_3$.[42] The strain hysteresis, quantified as the area within the strain versus electric-field curve, reflects domain motions at low electric fields but is almost negligible above 5 kV mm^{-1}. It should be noted that the strain hysteresis in the present material is smaller than that in Bi-based giant strain lead-free ceramics,[43] Generally, the small hysteresis correlates to a small dissipated energy E_{dis}, which is the integral of the polarization versus electric-field curve. Under unipolar loading with a field of 3 kV mm^{-1}, the current material renders a small E_{dis} of 21 kJ m^{-3}, a little smaller than 26 kJ m^{-3} of lead-based soft PZT ceramics and much smaller than 61 kJ m^{-3} of lead-free $(1\text{-}x)(0.8Bi_{1/2}Na_{1/2}TiO_3\text{-}0.2Bi_{1/2}K_{1/2}TiO_3)\text{-}xBiZn_{1/2}Ti_{1/2}O_3$ ($x = 0.04$) ceramics.[44] The small strain hysteresis as well as dissipated energy lends the current material good positioning accuracy and low heat generation during operation, extending this material to high frequency applications.[42]

An intriguing result rests with the temperature-insensitive strain behavior of the current material, as provided in **Figure 3**a. This behavior is observed from room temperature up to 175 °C, which is comparable to the well-known LF4T textured ceramics reported by Saito et al.[4] However, an extremely complex texturing technology is required for LF4T. Our result is in variance with the generally accepted hypothesis that temperature-stability cannot be obtained in randomly oriented KNN-based ceramics due to the presence of the PPT effect, e.g., the non-textured LF4 ceramics depicted in Figure 3b. The temperature-dependent strain behavior (in terms of normalized strain d_{33}*) of several representative piezoceramics is also provided in Figure 3b for comparison. It is noted that the strain variation of the CZ5 ceramics in the investigated temperature range is less than ±10% of its room-temperature value (indicated by shadows in Figure 3b), much better than the PZT5H ceramics[45] with a similar Curie point around 200 °C. Even compared with the PZT4[4] ceramics, which have a much higher Curie point at around 325 °C and are dedicated for applications requiring constant outputs, CZ5 outperforms slightly in terms of temperature stability. A still existing drawback lies in the fact that PZT requires a lower driving field for the same amount of strain, e.g., 4 kV mm^{-1} and 2 kV mm^{-1} are required for KNN and PZT, respectively, to achieve 0.13% unipolar strain. As for the Bi-based giant strain material, e.g., 0.92BNT-0.06BT-0.02KNN,[46] though much higher strain (≈0.32% at 6 kV mm^{-1}) is obtained around room temperature, a large decrease up to 60% in the strain level is observed at 175 °C.

The result of superior temperature-insensitivity is brought into compositional context by comparing CZ5 to materials with different contents of $CaZrO_3$. Figure 3c demonstrates that

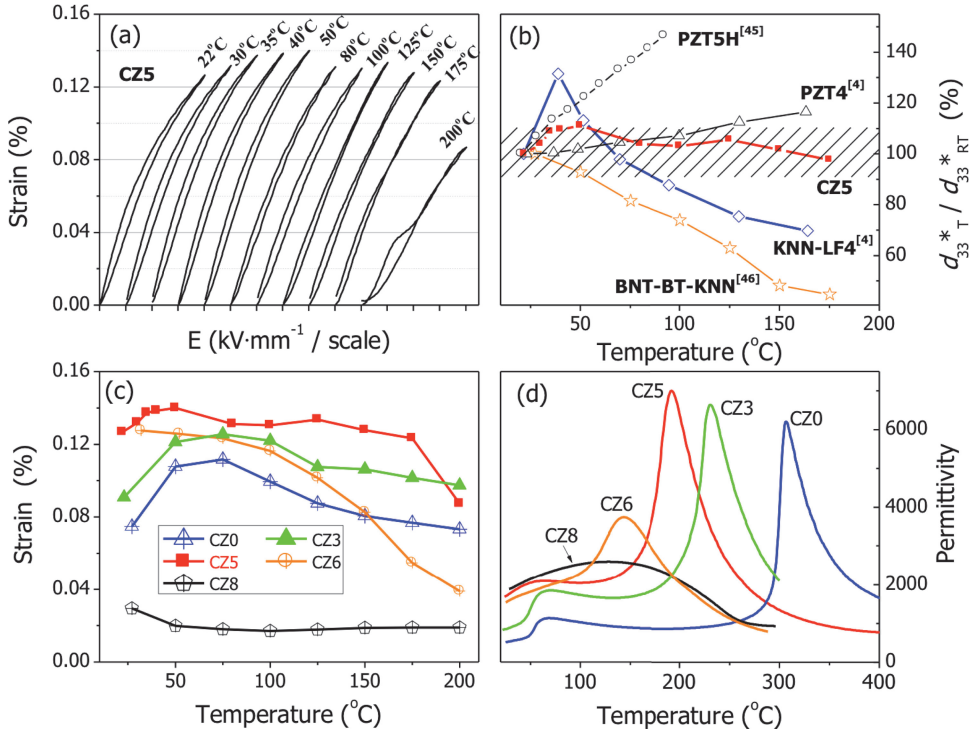

Figure 3. a) Temperature dependence of unipolar strain of CZ5 at 4 kV mm^{-1} field excursion. b) Comparison of temperature dependence of normalized strain d_{33}* for various piezoceramics as normalized to its room temperature value d_{33}*$_{RT}$. The data for PZT5H,[45] PZT4,[4] KNN-LF4,[4] BNT-BT-KNN[46] are taken from figures in the respective references. c) Temperature dependence of unipolar strain (at 4 kV mm^{-1}) of ceramics with different CZ content. d) Temperature dependence of permittivity (measured at 1 kHz) of poled samples with different CZ content.

© 2013 WILEY-VCH Verlag GmbH & Co. KGaA, Weinheim

the ceramic samples with other CZ contents do not exhibit temperature-stable strain behavior. For samples with lower CZ contents, e.g., CZ0 and CZ3, there are maxima in strain corresponding to permittivity shoulders as revealed in Figure 3d, which are considered a consequence of the PPT effect. For samples with higher CZ contents, strain values of CZ6 yield a monotonous decay with temperature due to a low Curie point around 150 °C, while CZ8 is characterized by a stable strain-temperature curve at very small strain values probably due to complete suppression of ferroelectric order. As the permittivity curve in Figure 3d reveals, CZ5 is gifted with the ideal phase structure with a small difference in free energy between orthorhombic and tetragonal phases such that the influence of PPT is mitigated. It may also be speculated that the phase transition temperature is a function of applied electric field as reported for BNT-based piezoceramics, diffusing the transition temperature further during field excursions.[47] At the same time, the Curie point is not too low, allowing the tetragonal phase to remain stable in a relatively wide temperature range. Actually, the phase structural evolutions of CZ5 with increasing temperatures, that from orthorhombic-tetragonal coexistence to tetragonal then finally to cubic, are verified by laboratory-level XRD measurements. However, the deviations between various phases are modest, which means that advanced facilities like synchrotron are preferred for detailed characterization.

2.3. Phenomenological Description

One may contemplate whether piezoelectric coefficient d_{33} of CZ5 could exhibit similar temperature-stable behavior as normalized strain d_{33}*; The temperature-dependent piezoelectric coefficient d_{33}, which is very rarely reported in KNN-based ceramics due to a shortage of commercial equipment, is measured here in situ by a custom-designed apparatus, with 10 V applied on a 1 mm thick sample.[48] The piezoelectric coefficient d_{33} at room temperature is in the range of 300–320 pm V^{-1}, comparable to that measured by a Berlincourt-type meter. With increasing temperature (see **Figure 4**a), d_{33} reveals a broad maximum centered at about 36 °C and then decreases gradually culminating in a significant drop near the Curie point T_C. This behavior is therefore consistent with a PPT at room temperature, as ascertained in the X-ray data as well with a broad phase transition regime as identified with the temperature-dependent dielectric properties lying between room temperature and 80 °C.

The change of piezoelectric coefficient d_{33} is also reflected in local PFM measurements.[49] The PFM method is based on the detection of local sample deformations induced by a weak ac field. For the vertical PFM, the measured signal, D_{loc}, is proportional to the longitudinal piezoelectric coefficient d_{33} inside a single domain. D_{loc} can be estimated from profiles of the PFM signal taken across two neighboring antiparallel domains (see details in Figure S4, Supporting Information). Figure 4b provides temperature dependences $D_{loc}(T)$ obtained for several representative profiles taken in regions exhibiting maximal VPFM signal at room temperature. These dependences are in good accordance with the plot in Figure 4a indicating qualitative similarity in piezoelectric coefficient d_{33} macroscopic behavior and

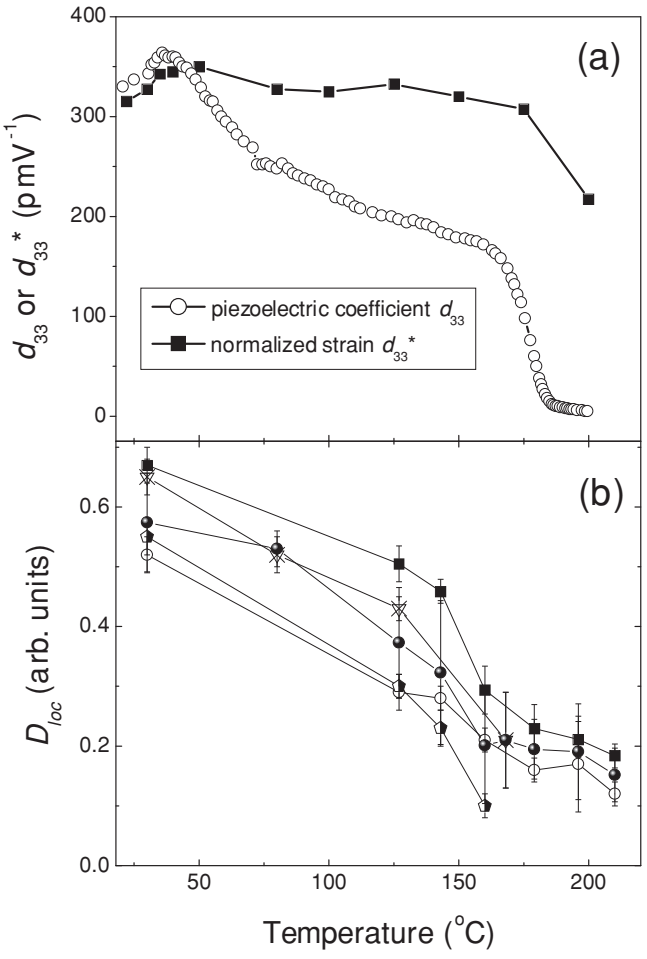

Figure 4. a) Temperature dependence of in situ measurement of small signal d_{33} and large signal d_{33}*. The d_{33}* is calculated according to the unipolar strain at 4 kV mm^{-1}. b) Change of the local piezoresponse inside individual domains obtained from the PFM study.

local single domain. Details of the calculation of parameter D_{loc} in Figure 4b are explicated in Supporting Information.

In contrast, the normalized strain d_{33}*, which is derived from unipolar strain, remains almost constant in the range of 300–350 pmV^{-1} from room temperature up to 175 °C. Note that the small value of the normalized strain d_{33}*, compared to the piezoelectric coefficient d_{33} at room temperature, stems from the large chosen field amplitude, but is higher, e.g., for 1 kV mm^{-1} with a value of 400 pmV^{-1} (Figure S3, Supporting Information). The different temperature-dependent behavior of d_{33}* could be rationalized using the phenomenological relationship of electrostriction in ferroelectrics. For a better understanding of this phenomenon, temperature-dependent polarization (P–E) as well as bipolar strain hysteresis loops were measured, as presented in **Figure 5**. Well-saturated P–E loops are observed for all temperatures at 4 kV mm^{-1}. The temperature dependence of various parameters, e.g., unipolar strain S_{uni}, remanent polarization P_r, etc., are summarized in **Figure 6**.

For tetragonal piezoelectrics, the piezoelectric coefficient d_{33} is determined by the following equation,[50]

© 2013 WILEY-VCH Verlag GmbH & Co. KGaA, Weinheim

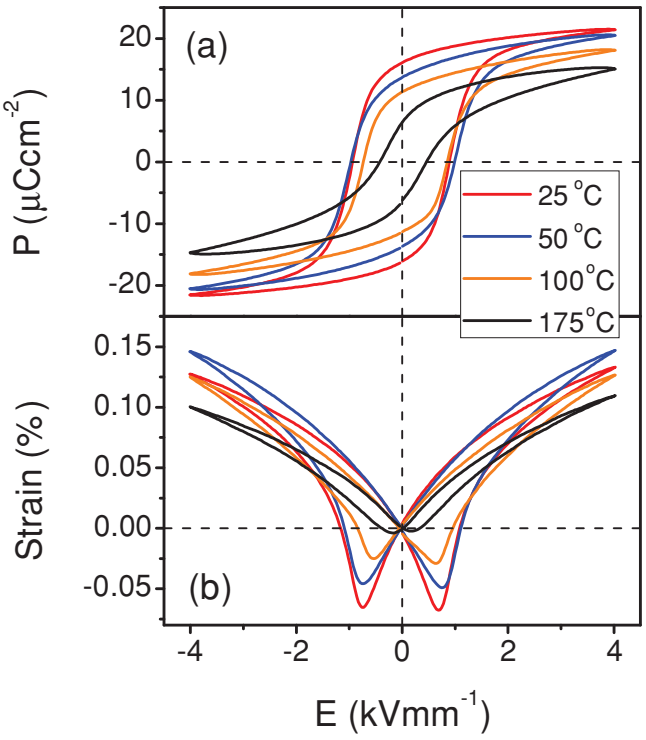

Figure 5. a) Polarization hysteresis loops and b) bipolar strain curves of CZ5 measured at 25 °C, 50 °C, 100 °C, and 175 °C.

$$d_{33} = 2Q\varepsilon_0\varepsilon_{33}P_3 \quad (1)$$

where Q is the electrostrictive constant and typically varies little with temperature;[51] ε_0 is the vacuum permittivity; ε_{33} is the permittivity and in this case it does not change much before T_C, as shown in Figure 3d. However, P_3 is the polarization along the polar axis and approximately equals remanent polarization P_r for ferroelectric ceramics, which in this case decreases almost linearly with increasing temperature, as displayed in Figure 6. Strictly, the P_3 in Equation 1, which is related to the piezoelectric coefficient d_{33}, is not exactly the P_r measured by means of Figure 5, due to the existence of temperature-dependent thermal depoling and time-dependent relaxation; in this case, P_3 decays more severely than P_r. The piezoelectric coefficient d_{33} reaches a small peak as shown in Figure 4a, due to the permittivity anomaly around $T_{O\text{-}T}$; then it follows the decreasing trend of remanent polarization and finally suffers a sudden drop before T_C.

The normalized strain d_{33}* is derived from the unipolar strain at a certain electric field. For a succinct understanding, the electrostrictive behavior as relationship between field-induced strain S and polarization P is considered,[52] as Equation 2:

$$S = QP^2 \quad (2)$$

where Q is the electrostrictive constant. Note that this equation is valid not only for pure electrostrictors but also for other materials showing electrostrictive behaviors, e.g., ferroelectric piezoelectrics.[53] Considering unipolar field excursions, we obtain the unipolar strain S_{uni} as related to the remanent and maximum polarization as written in Equation 3:[54]

$$S_{uni} = S_{max} - S_{rem} = QP_{max}^{2-}QP_r^2 = Q(P_{max}^{2-}P_r^2) \quad (3)$$

where P_{max} is the maximum electric-field-induced polarization and P_r is the remanent polarization. P_{max} and P_r can both be obtained in the P–E loop as provided in Figure 5a. The temperature dependence of S_{uni} and P_{max}^2–P_r^2 are contrasted in Figure 6, exhibiting exactly the same traces, hence validating Equation 3. The temperature dependence of P_{max} and P_r are also provided in Figure 6. It is concluded that the temperature-insensitive unipolar strain behavior in the present study is due to the constant values of the difference of squared values of P_{max} and P_r, or P_{max}^2–P_r^2, with temperature variation below the Curie point T_C. Therefore, a reduction in P_{max} with temperature can be compensated by a stronger reduction in P_r with temperature, yielding a temperature-insensitive unipolar strain.

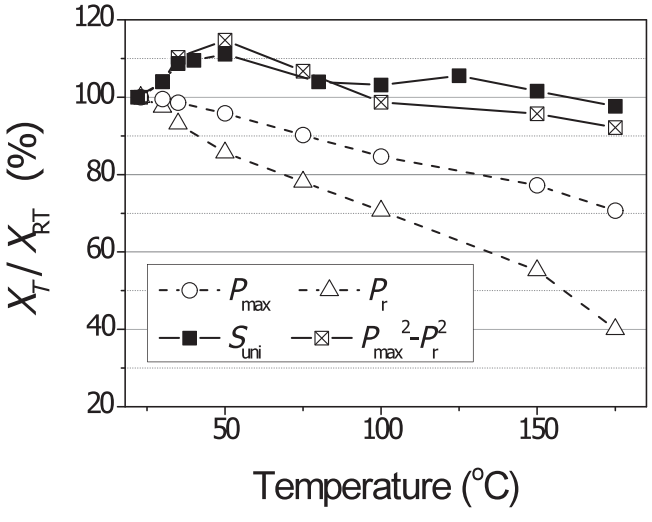

Figure 6. Temperature stability of various parameters. X_T and X_{RT} signify P_{max}, P_r, S_{uni} and $P_{max}^2 - P_r^2$ at different temperatures.

3. Conclusions

We have developed a new lead-free KNN-based piezoceramic with temperature-insensitive strain behavior. A high level of unipolar strain up to 0.16% is obtained at room temperature, with slim hysteresis and dissipated energy even smaller than PZT ceramics. The electric field-induced strain is found to vary less than 10% in the temperature regime from room temperature up to 175 °C. These excellent features render the current material especially suitable for high-precision actuator applications demanding good temperature stability. The origin of this temperature-insensitive unipolar strain behavior in the present study is phenomenologically attributed to the stable difference of squared values of P_{max} and P_r over a wide temperature range, based on Equation 3. It is believed that a series of KNN-based ceramics, given that the free energy barrier between orthorhombic and tetragonal phases is tuned, will present similar temperature-insensitive strain behavior.

© 2013 WILEY-VCH Verlag GmbH & Co. KGaA, Weinheim

4. Experimental Section

Ceramic samples with composition $(1\text{-}x)(Na_{0.49}K_{0.49}Li_{0.02})(Nb_{0.8}Ta_{0.2})O_3\text{-}xCaZrO_3$ (abbreviated as CZ*x*), with 2 wt% MnO_2 addition, were prepared by a conventional ceramic processing route. The oxides or carbonates (all Alfa Aesar GmbH & Co. KG, Karlsruhe, Germany) of the respective elements, namely Li_2CO_3 (99.0%), Na_2CO_3, (99.5%), K_2CO_3 (99.0%), Nb_2O_5 (99.9%), Ta_2O_5 (99.0%), $CaCO_3$ (99.5%), ZrO_2 (99.5%), MnO_2 (99.5%) were mixed according to a stoichiometric ratio with the nominal composition, followed by ball milling for 24 h in an ethanol solution. The mixed powders were calcined at 900 °C for 4 h and subjected to ball milling again for 24 h to enhance the compositional homogenization. The synthesized powders were then pressed into disks of 10 mm in diameter and 1.5 mm in thickness, followed by cold-isostatic pressing under 300 MPa. Such pellets were sintered in air at 1080–1120 °C for 2 h. High-resolution XRD measurements with Cu Kα radiation (Rigaku, D/Max 2500) were carried out to determine the crystal phase. Samples were poled under 3 kV mm^{-1} bias at 80 °C in a silicone oil bath for 30 min.

For the macroscopic electrical characterization, pellets were ground down to 1 mm height and painted with silver paste that was burnt in afterwards at 400 °C to form the electrodes. Permittivity and dielectric loss were measured as a function of temperature using an impedance analyzer (HP 4192A, Palo Alto, CA). The piezoelectric coefficient d_{33} was checked at room temperature using a quasi-static piezoelectric constant testing meter (ZJ-3A, Institute of Acoustics, Chinese Academy of Science), and also determined in situ as a function of temperature by a custom-designed apparatus, which is described in detail elsewhere.[48] The normalized strain $d_{33}*$ as well as polarization-electric field (*P*–*E*) hysteresis loops were measured using a ferroelectric tester (aixACC TF Analyzer 2000) at various temperatures, with a fixed frequency of 1 Hz.

The TEM specimen was obtained by mechanically polishing to a thickness of about 20 μm. The central parts of the disks were further reduced by precision argon-ion milling (RES101, Leica EM, Wetzlar, Germany) at an acceleration voltage of 6 kV. These specimens were investigated using a high-resolution TEM (HRTEM JEOL 2011) operated at 200 kV with a point resolution of 0.19 nm.

For the PFM observations the sintered samples were ground down to about 250 μm and subsequently polished using polycrystalline diamond paste with abrasive particles of 15 μm, 6 μm, 3 μm and 1 μm (DP-Paste P by Struers A/S, Ballerup, Denmark) for 1 h each. The PFM experiments were carried out using a commercial atomic force microscopy MFP-3D (Asylum Research, USA). The PFM signal was obtained under ac voltage U_{ac} = 5-10 V, f_{ac} = 50 kHz applied to a conductive Pt-Ir coated cantilever PPP-NCHPt (Nanosensors, Switzerland). The measurements were done in the temperature range from 25 °C up to 220 °C. Both vertical and lateral PFM images were taken, which provide information about the distribution of out-of-plane and in-plane components of polarization, respectively. The PFM images were analyzed using WSxM software (Nanotec Electronica, Spain).[55]

Supporting Information

Supporting Information is available from the Wiley Online Library or from the author.

Acknowledgements

K.W. acknowledges the Alexander von Humboldt foundation for a fellowship. This work was also supported by the National Nature Science Foundation of China (Grant No. 51211140345) and 973 Program (Grant. No. 2009CB623304). Part of this work was performed in the framework of the EU Marie Curie International Training Network "Nanomotion".

Received: December 18, 2012
Revised: January 30, 2013
Published online: March 19, 2013

[1] K. Uchino, *Piezoelectric actuators and ultrasonic motors*, Kluwe, Boston **1997**.
[2] E. Cross, *Nature* **2004**, *432*, 24.
[3] W. Jo, R. Dittmer, M. Acosta, J. Zang, C. Groh, E. Sapper, K. Wang, J. Rödel, *J. Electroceram.* **2012**, *29*, 71.
[4] Y. Saito, H. Takao, T. Tani, T. Nonoyama, K. Takatori, T. Homma, T. Nagaya, M. Nakamura, *Nature* **2004**, *432*, 84.
[5] T. Takenaka, H. Nagata, *J. Eur. Ceram. Soc.* **2005**, *25*, 2693.
[6] T. R. Shrout, S. J. Zhang, *J. Electroceram.* **2007**, *19*, 111.
[7] J. Rödel, W. Jo, K. T. P. Seifert, E. M. Anton, T. Granzow, D. Damjanovic, *J. Am. Ceram. Soc.* **2009**, *92*, 1153.
[8] W. Liu, X. Ren, *Phys. Rev. Lett.* **2009**, *103*, 257602.
[9] K. Wang, J.-F. Li, *Adv. Funct. Mater.* **2010**, *20*, 1924.
[10] T. Sluka, A. K. Tagantsev, D. Damjanovic, M. Gureev, N. Setter, *Nat. Commun.* **2012**, *3*, 748.
[11] I. Levin, I. M. Reaney, *Adv. Funct. Mater.* **2012**, *22*, 3445.
[12] D. Schütz, M. Deluca, W. Krauss, A. Feteira, T. Jackson, K. Reichmann, *Adv. Funct. Mater.* **2012**, *22*, 2285.
[13] L. Egerton, D. M. Dillon, *J. Am. Ceram. Soc.* **1959**, *42*, 438.
[14] Y. P. Guo, K. Kakimoto, H. Ohsato, *Appl. Phys. Lett.* **2004**, *85*, 4121.
[15] E. Hollenstein, M. Davis, D. Damjanovic, N. Setter, *Appl. Phys. Lett.* **2005**, *87*, 182905.
[16] Y. J. Dai, X. W. Zhang, G. Y. Zhou, *Appl. Phys. Lett.* **2007**, *90*, 262903.
[17] E. K. Akdoğan, K. Kerman, M. Abazari, A. Safari, *Appl. Phys. Lett.* **2008**, *92*, 112908.
[18] J. Fu, R. Zuo, Z. Xu, *Appl. Phys. Lett.* **2011**, *99*, 062901.
[19] K. Wang, J.-F. Li, *Appl. Phys. Lett.* **2007**, *91*, 262902.
[20] S. J. Zhang, R. Xia, T. R. Shrout, G. Z. Zang, J. F. Wang, *J. Appl. Phys.* **2006**, *100*, 104108.
[21] K. Wang, J.-F. Li, N. Liu, *Appl. Phys. Lett.* **2008**, *93*, 092904.
[22] T. A. Skidmore, T. P. Comyn, S. J. Milne, *Appl. Phys. Lett.* **2009**, *94*, 222902.
[23] D. W. Baker, P. A. Thomas, N. Zhang, A. M. Glazer, *Appl. Phys. Lett.* **2009**, *95*, 091903.
[24] J. Tellier, B. Malic, B. Dkhil, D. Jenko, J. Cilensek, M. Kosec, *Solid State Sci.* **2009**, *11*, 320.
[25] N. Klein, E. Hollenstein, D. Damjanovic, H. J. Trodahl, N. Setter, M. Kuball, *J. Appl. Phys.* **2007**, *102*, 014112.
[26] W. Ge, Y. Ren, J. Zhang, C. P. Devreugd, J. Li, D. Viehland, *J. Appl. Phys.* **2012**, 111.
[27] S. J. Zhang, R. Xia, T. R. Shrout, *Appl. Phys. Lett.* **2007**, *91*, 132913.
[28] E. Hollenstein, D. Damjanovic, N. Setter, *J. Eur. Ceram. Soc.* **2007**, *27*, 4093.
[29] J. G. Wu, D. Q. Xiao, Y. Y. Wang, W. J. Wu, B. Zhang, J. G. Zhu, *J. Appl. Phys.* **2008**, *104*, 024102.
[30] Y. Chang, S. Poterala, Z. Yang, G. L. Messing, *J. Am. Ceram. Soc.* **2011**, *94*, 2494.
[31] S.-Y. Choi, S.-J. Jeong, D.-S. Lee, M.-S. Kim, J.-S. Lee, J. H. Cho, B. I. Kim, Y. Ikuhara, *Chem. Mater.* **2012**, *24*, 3363.
[32] R. Zuo, J. Fu, *J. Am. Ceram. Soc.* **2011**, *94*, 1467.
[33] R. P. Herber, G. A. Schneider, S. Wagner, M. J. Hoffmann, *Appl. Phys. Lett.* **2007**, *90*, 252905.
[34] K. Wang, J.-F. Li, *J. Am. Ceram. Soc.* **2010**, *93*, 1101.
[35] S. Zhang, H. J. Lee, C. Ma, X. Tan, *J. Am. Ceram. Soc.* **2011**, *94*, 3659.
[36] J. J. Yao, J. F. Li, D. Viehland, Y. F. Chang, G. L. Messing, *Appl. Phys. Lett.* **2012**, *100*, 132902.
[37] K. A. Schonau, L. A. Schmitt, M. Knapp, H. Fuess, R. A. Eichel, H. Kungl, M. J. Hoffmann, *Phys. Rev. B* **2007**, *75*, 184117.
[38] R. Theissmann, L. A. Schmitt, J. Kling, R. Schierholz, K. A. Schonau, H. Fuess, M. Knapp, H. Kungl, M. J. Hoffmann, *J. Appl. Phys.* **2007**, *102*, 024111.
[39] G. A. Rossetti, A. G. Khachaturyan, G. Akcay, Y. Ni, *J. Appl. Phys.* **2008**, *103*, 114113.
[40] F. M. Bai, J. F. Li, D. Viehland, *J. Appl. Phys.* **2005**, *97*, 054103.

© 2013 WILEY-VCH Verlag GmbH & Co. KGaA, Weinheim

[41] S. Wada, K. Yako, H. Kakemoto, T. Tsurumi, T. Kiguchi, *J. Appl. Phys.* **2005**, *98*, 014109.
[42] S. E. Park, T. R. Shrout, *J. Appl. Phys.* **1997**, *82*, 1804.
[43] S. T. Zhang, A. B. Kounga, E. Aulbach, H. Ehrenberg, J. Rödel, *Appl. Phys. Lett.* **2007**, *91*, 112906.
[44] R. Dittmer, W. Jo, J. Daniels, S. Schaab, J. Rödel, *J. Am. Ceram. Soc.* **2011**, *94*, 4283.
[45] D. Wang, Y. Fotinich, G. P. Carman, *J. Appl. Phys.* **1998**, *83*, 5342.
[46] S. T. Zhang, A. B. Kounga, E. Aulbach, W. Jo, T. Granzow, H. Ehrenberg, J. Rödel, *J. Appl. Phys.* **2008**, *103*, 034108.
[47] E. Sapper, S. Schaab, W. Jo, T. Granzow, J. Rödel, *J. Appl. Phys.* **2012**, *111*, 014105.
[48] T. Leist, J. Chen, W. Jo, E. Aulbach, J. Suffner, J. Rödel, *J. Am. Ceram. Soc.* **2012**, *95*, 711.
[49] R. Dittmer, W. Jo, J. Rödel, S. Kalinin, N. Balke, *Adv. Funct. Mater.* **2012**, *22*, 4208.
[50] D. Damjanovic, *J. Am. Ceram. Soc.* **2005**, *88*, 2663.
[51] J. Kuwata, K. Uchino, S. Nomura, *Jpn. J. Appl. Phys.* **1980**, *19*, 2099.
[52] K. Uchino, S. Nomura, L. E. Cross, R. E. Newnham, S. J. Jang, *J. Mater. Sci.* **1981**, *16*, 569.
[53] W. Heywang, K. Lubitz, W. Wersing, *Piezoelectricity: Evolution and Future of a Technology*, Springer, Heidelberg **2008**.
[54] W. Jo, T. Granzow, E. Aulbach, J. Rödel, D. Damjanovic, *J. Appl. Phys.* **2009**, *105*, 094102.
[55] I. Horsas, R. Fernández, J. M. Gómez-Rodriguez, J. Colchero, J. Gómez-Herrero, A. M. Baro, *Rev. Sci. Instrum.* **2007**, *78*, 013705.

© 2013 WILEY-VCH Verlag GmbH & Co. KGaA, Weinheim